



# 1 Ship-borne lidar measurements showing the progression of the 2 tropical reservoir of volcanic aerosol after the June 1991 Pinatubo 3 eruption.

4 Juan-Carlos Antuña-Marrero<sup>1</sup>, Graham W. Mann<sup>2,3</sup>, Philippe Keckhut<sup>4</sup>, Sergey Avdyushin<sup>5†</sup>, Bruno  
5 Nardi<sup>6</sup> and Larry W. Thomason<sup>7</sup>

6 <sup>1</sup>Departamento de Física Teórica, Atómica y Óptica, Universidad de Valladolid, 47002, España

7 <sup>2</sup>School of Earth and Environment, University of Leeds, Leeds, LS2 9JT, UK.

8 <sup>3</sup>National Centre for Atmospheric Science (NCAS-Climate), University of Leeds, Leeds, UK

9 <sup>4</sup>Laboratoire Atmosphères, Milieux, Observations Spatiales, Université de Versailles Saint-Quentin, Versailles, 78280, France

10 <sup>5</sup>Fedorov Institute of Applied Geophysics, Moscow, Russia

11 <sup>6</sup>Nardi Scientific, LLC, Denver, CO, USA.

12 <sup>7</sup>NASA Langley Research Center, Hampton, Virginia, USA

13 †Deceased

14

15 *Correspondence to:* Juan-Carlos Antuña-Marrero ([antuna@goa.uva.es](mailto:antuna@goa.uva.es))

16

## 17 **Abstract:**

18 A key limitation of volcanic forcing datasets for the Pinatubo period, is the large uncertainty that remains with respect to the  
19 extent of the optical depth of the Pinatubo aerosol cloud in the first year after the eruption, the saturation of the SAGE-II  
20 instrument restricting it to only be able to measure the upper part of the aerosol cloud in the tropics. Here we report the recovery  
21 of stratospheric aerosol measurements from two ship-borne lidars, both of which measured the tropical reservoir of volcanic  
22 aerosol produced by the June 1991 Mount Pinatubo eruption. The lidars were on-board two Soviet vessels, each ship crossing  
23 the Atlantic, their measurement datasets providing unique observational transects of the Pinatubo cloud across the tropics from  
24 Europe to the Caribbean (~40°N to 8°N) from July to September 1991 (the Prof Zubov ship) and from Europe to south of the  
25 Equator (8°S to ~40°N) between January and February 1992 (the Prof Vize ship). Our philosophy with the data recovery is to  
26 follow the same algorithms and parameters appearing in the two peer-reviewed articles that presented these datasets in the same  
27 issue of GRL in 1993, and here we provide all 48 lidar soundings made from the Prof. Zubov, and 11 of the 20 conducted from  
28 the Prof. Vize, ensuring we have reproduced the aerosols backscatter and extinction values in the Figures of those two papers.  
29 These original approaches used thermodynamic properties from the CIRA-86 standard atmosphere to derive the molecular  
30 backscattering, vertically and temporally constant values applied for the aerosol backscatter to extinction ratio and the  
31 correction factor of the aerosols backscattering wavelength dependence. We demonstrate this initial validation of the recovered  
32 stratospheric aerosol extinction profiles, providing full details of each dataset in this paper's Supplement S1. We anticipate the  
33 data providing potential new observational case studies for modelling analyses, including a 1-week series of consecutive  
34 soundings (in September 1991) at the same location showing the progression of the entrainment of part of the Pinatubo plume  
35 into the upper troposphere and the formation of an associated cirrus cloud.. The Zubov lidar dataset illustrates how the



36 tropically confined Pinatubo aerosol cloud transformed from a highly heterogeneous vertical structure in August 1991,  
37 maximum aerosol extinction values around 19 km for the lower layer and 23-24 for the upper layer, to a more homogeneous  
38 and deeper reservoir of volcanic aerosol in September 1991. We encourage modelling groups to consider new analyses of the  
39 Pinatubo cloud, comparing to the recovered datasets, with the potential to increase our understanding of the evolution of the  
40 Pinatubo aerosol cloud and its effects. Data described in this work , the original text files of the aerosols backscatter ratio, the  
41 calculated aerosols backscatter and aerosols extinction profiles are available at  
42 <https://doi.pangaea.de/10.1594/PANGAEA.912770> (Antuña-Marrero et al., 2020).

43



## 44 1. Introduction

45 Observations by satellite and in situ measurements showed that major volcanic eruptions enhance the stratospheric aerosol  
46 layer for several years (Stratospheric Processes and their Role in Climate -SPARC, 2006). Such enhancement causes radiative,  
47 thermal, dynamical and chemical perturbations in different regions of the earth's atmosphere, resulting in a perturbation of the  
48 earth's climate (e.g. Robock, 2000; Timmreck, 2012). Current research on those perturbations demand detailed information  
49 about the 3D spatial and temporal distributions of stratospheric aerosols both under background conditions and after the  
50 volcanic eruptions. The June 1991 Mt. Pinatubo eruption is the most used for such research activities because it has been the  
51 largest and best documented eruption for the XX century up to the present. Still there are notable gaps in the information  
52 collected because the lack of enough measurements but also because several of the measurements conducted and reported in  
53 the literature have not been shared by the scientist and institutions that conducted them.

54 This work is a contribution to the Data Rescue Activity of the Stratospheric Sulfur and its Role in Climate (SSiRC) recently  
55 included in this SPARC initiative. This data rescue activity is aimed to "...foster new collaborations between scientists to  
56 recover, re-digitize and re-calibrate other historic stratospheric aerosol data sets, and invite scientists to contribute to this  
57 activity and to provide advice and expertise on how best to recover other incomplete long term observations of stratospheric  
58 composition," (SSiRC, 2020). In its current initial stage particular attention to gather datasets to characterize the progression  
59 of the aerosol cloud during the initial months after the 1991 Pinatubo eruption, the main motivation for the work we present  
60 here.

61 Among the envisaged applications of the two Mt Pinatubo's stratospheric aerosols lidar datasets we are presenting is the  
62 contribution to future improvements of the Global Space-based Stratospheric Aerosol Climatology, (GloSSAC). GloSSAC is  
63 the most complete source of information about the global spatial and temporal distribution of the stratospheric aerosols optical  
64 properties from 1979 to the present (Thomasson et al., 2018). From 1979 to mid-2005 the climatology relies mainly on the  
65 observations from the Stratospheric Aerosol and Gas Experiment (SAGE) series of satellite instruments. Only two lidar datasets  
66 in the tropics were used for filling the gap in SAGE II aerosols extinction profiles in this region in GloSSAC (Thomasson et  
67 al., 2018), produced by the dense stratospheric aerosols layer (McCormick and Veiga, 1992).

68 In section 2 the datasets are briefly described, providing the detailed description, format and inventory of the datasets contained  
69 on Supplement S1. Following section 3 describe the processing conducted to try to reproduce the values of the aerosol's  
70 extinction profiles at 532 nm for both ship borne lidars Zubov and Vize respectively. Section 4 show and discuss the results  
71 comparing them with the available information reported in Avdyushin et al, (1991) and Nardi et al., (1991). The section includes



72 the discussion of several features of the stratospheric aerosols from Mt. Pinatubo eruption during the period the measurements  
73 were taken to illustrate the importance of the rescued datasets. Follows section 5 showing an application of the reconstructed  
74 dataset in the validation of Mt Pinatubo modeling simulations. The article conclude with the summary and outlook.

75

## 76 2. Aerosols Scattering Ratio Datasets

77

### 78 2.1 Lidar datasets:

79 Here we report the two sets of scattering ratio profiles measured by two Soviet ship borne lidars a few months after the Mt  
80 Pinatubo June 1991 eruption across the north Atlantic Ocean. Professor Zubov ship carried a lidar from July to September  
81 1991, and Professor Vize, in January and February 1992 (Avdyushin et al., 1993; Nardi et al., 1993). The measurements  
82 campaign was part of a joint effort between the Roscomhydromet of the former Soviet Union and the Service d'Aeronomie du  
83 CNRS of France. It included another ship borne lidar on the French military ship Henry Poincare, based in Brest, and two  
84 ground based lidars. The lidars were located at the Observatory of Haute-Provence (OHP: 44 °N, 6 °E) and at the Centre  
85 d'Essai des Landes at Biscarosse (CEL: 44 °N, 1°W). A broad description appears in Nardi et al., (1993) and Avdyushin et al.,  
86 (1993).

87 Because of the particular spatio temporal distribution of the lidar measurements from Zubov they contribute in characterizing  
88 the variability of the Mt Pinatubo stratospheric aerosols (SA) vertical extinction profiles at certain points and regions of the  
89 North Atlantic Ocean between July and September 1991. Spatially the variability covers both latitudinal and longitudinal and  
90 temporally the daily variability of two Atlantic locations where lidar measurements were conducted for several consecutive  
91 and nonconsecutive days.

92 **Table 1: Technical features of the two ship borne lidars. Ya: Yttrium-aluminum. From table 1 Avdyushin et al., (1991)**

<b>Lidar Technical Features</b>	<b>Professor Zubov</b>	<b>Professor Vize</b>
Laser type	Doubled-Ya	Dye:R6W
Wavelength (nm)	539.5	589
Energy/pulse (J)	0.2	0.4
Frequency (s <sup>-1</sup> )	25	5
Power (W)	5	2
Emitted Beam Width (rad)	5 x 10 <sup>-4</sup>	5 x 10 <sup>-4</sup>
Receiver telescope diameter (cm)	110	110
Filter FWHH (nm)	0.5	0.8
Vertical resolution (m)	150	300

93



## 94 2.2 Data source

95 Prof Philippe Keckhut contributed the lidar scattering ratios (SR) profiles dataset derived from the lidar measurements  
96 conducted by Zubov and Vize vessels for the PhD dissertation research of the lead author in 1999. The goal of that research  
97 was to validate the Mt Pinatubo SA extinction profiles measured by the Stratospheric Aerosols and Gas Experiment II (SAGE  
98 II) with ground based lidar observations (Antuña et al., 2002; 2003). However, we found very low information to comply with  
99 the proposed goal due to the combination of two facts. Firstly, the SAGE II profiles were truncated above the main core of the  
100 SA layer in the tropics during almost half a year after the June 1991 Mt Pinatubo eruption. It was the result of the elevated  
101 atmospheric opacity produced by the SA (McCormick and Veiga, 1992). Secondly the few coincident vessel's lidar and SAGE  
102 II extinction profiles measurements, because of the coincidence criteria selected (Antuña et al, 2002). The dataset was not used  
103 and remained stored in the lead author archives since then.

104

## 105 2.3 Dataset description

106 In brief, the datasets consist of 48 data files from the Professor Zubov vessel containing daily profiles of the lidar SR(z) profiles  
107 and 11 lidar SR(z) profiles from Professor Vize vessel. It should be taken into account that in the case of the Vize lidar we  
108 have only 11 of the 20 measurements reported to be conducted (Avdyushin et al., 1993; Nardi et al., 1993).

109

## 110 3. Data processing

111 To comply with the goal to reproduce the aerosols extinction vertical profiles ( $\alpha_{\text{ext}}(z)$ ) reported in Avdyushin et al., (1993) and  
112 Nardi et al., (1993) from the available SR(z), we used the same algorithms and parameters they mention. They used the  
113 Rayleigh backscattering cross section coefficient of  $5.7 \times 10^{-32} \text{ m}^2 \text{ sr}^{-1}$  at 532 nm. In the case of Zubov no wavelength dependence  
114 was accounted for considering negligible the differences between the 532 nm and 539 nm. A correction factor of the Rayleigh  
115 backscattering cross section coefficient at 532 nm ( $589^4/532^4 = 0.666$ ) considering the 589 nm of VIZE data, was used  
116 (Avdyushin et al., 1991)

117 Then Rayleigh backscatter at the surface was calculated and for each lidar measurement the Rayleigh backscatter profiles  
118 ( $\beta_{\text{mol}}(z)$ ) were derived using the vertical profiles of pressure (P(z)), and temperature (T(z)) from the CIRA-86 atmospheric  
119 model (Flemming et al., 1988). The procedure consisted in determining the geopotential height (Zg(z)) and T(z) at the  
120 mandatory P(Z) levels from 1000 to 0.1 hPa from the CIRA-86 atmosphere taking into account the month the measurement



121 was conducted and latitude of the ship for each individual measurement. Then the  $Z_g(z)$  were converted to geometric altitude  
122 ( $z$ ). Following the  $P(z)$  were logarithmically interpolated in the vertical to the altitude of the lidar SR levels. Similar step was  
123 conducted for  $T(z)$  but using lineal interpolation. Then the  $\beta_{mol}(z)$  is derived using the standard procedure (Bucholtz, 1995).  
124 Following the aerosols backscattering profiles ( $\beta_{aer}(z)$ ) were derived using equation 1 (Russell et al., 1979). To avoid zero or  
125 negative values in  $\beta_{aer}(z)$ , produced by  $SR(z)$  equal or lower than 1 respectively, we replaced those  $SR(z)$  values by 1.01  
126 following, the value proposed by Russell et al., (1979) for the  $SR(z)$  minimum aerosol level. At the levels where this change  
127 took place the magnitude of  $\beta_{aer}(z)$  is two orders lower than the magnitude of  $\beta_{mol}(z)$  at the same level. Equation 1 was used to  
128 derive  $\beta_{aer}(z)$ :

$$129 \quad \beta_{aer}(z) = [SR(z) - 1] \times \beta_{mol}(z) \quad (1)$$

130 The next step consisted in calculating the  $\alpha_{aer}(z)$  from the  $\beta_{aer}(z)$  using equation 2, using a constant value in time and altitude  
131 of  $0.04 \text{ sr}^{-1}$  for the aerosols backscattering to extinction ratio (Advuyshin et al., 1991).

$$132 \quad \alpha_{aer}(z) = \beta_{aer}(z) \left[ \frac{\beta_{aer}}{\alpha_{aer}} \right]^{-1} \quad (2)$$

133

## 134 4. Results

135 The tabulated lidar SR profiles and the calculated  $\beta_{aer}(z)$  and  $\alpha_{aer}(z)$  profiles at the wavelength of 532 nm from both lidars are  
136 available at <https://doi.pangaea.de/10.1594/PANGAEA.912770> (Antuña-Marrero et al., 2020).

137

### 138 4.1 Validation of the reproduced dataset

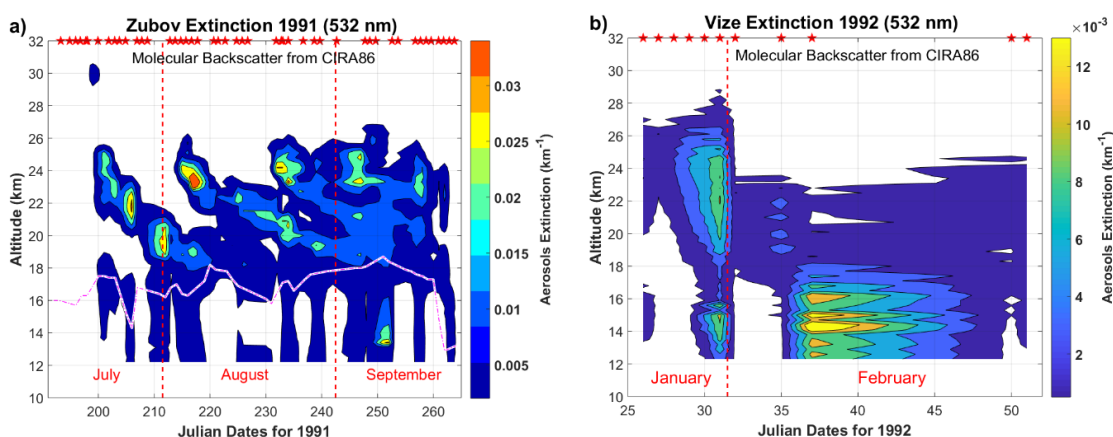
139 No tabulated data is available for the  $\alpha_{aer}(z)$  values used in the cited Advuyshin or Nardi's papers, the only published source of  
140 information about the measurements. In addition, the papers do not conduct detailed discussions or mentions of the extinction  
141 relevant features in the Zubov and Vize datasets. Here we make use of all the available information to conduct a semi-  
142 quantitative validation for the Zubov dataset. In the case of Vize only is possible to conduct a qualitative validation.

143 Figures 1a and 1b show the temporal/vertical cross section of the  $\alpha_{aer}(z)$  measured by the lidars onboard the Professors Zubov  
144 and Vize ships. The black discontinuous line on top of the white background in figure 1a is the altitude of tropopause at the  
145 locations the lidar measurements were conducted. The tropopause altitudes were derived from the ERA-Interim reanalysis



146 potential vorticity profiles, interpolating to the height levels of the lidar measurements and select the height of the  $1.e-5$  PV  
147 surface.

148 Figure 1a shows, the same pattern of the temporal/vertical cross section of the  $\alpha_{\text{aer}}(z)$  for the entire Zubov trajectory that the  
149 one reported in figure 2 in Avdyushin et al., (1993). The magnitudes of the  $\alpha_{\text{aer}}(z)$  are in the same order in both figures as it  
150 could be seen comparing the scales of the color bars in the right side of both them. A careful comparison between the areas  
151 painted in red (corresponding to the highest values of  $\alpha_{\text{aer}}(z)$ ) in both figures show a larger area in Avdyushin et al, (1991)  
152 figure 2, an indication of slightly lower values in the values of  $\alpha_{\text{aer}}(z)$  we reproduced. Moreover, the maximum  $\alpha_{\text{aer}}(z)$  value in  
153 the reproduced dataset is  $0.054 \text{ km}^{-1}$  at 23.3 km of altitude on August 4<sup>th</sup> could be appreciated on figure 2a. Avdyushin et al,  
154 (1991) reported the maximum at 18 °N between 23 and 24 km of altitude with an  $\alpha_{\text{aer}}(z)$  value of  $0.08 \text{ km}^{-1}$  the same day. All  
155 those facts demonstrate the agreement of the reproduced dataset with the original one.



156

157 **Figure 1: Temporal/vertical cross sections of the aerosols extinction at 532 nm measured by the lidar onboard the two ship borne**  
158 **lidars during their trajectories. a) Professor Zubov ship; b) Professor Vize ship.**

159

160 In the figure 1a it should be also noted the presence of area of high values of the  $\alpha_{\text{aer}}(z)$  at the tropical middle troposphere in  
161 September 1991 around the day 250. This signature is not seen on the temporal cross section from Zubov lidar on figure 2 in  
162 Avdyushin et al., (1991) because the vertical axes lower altitude is at 15 km. It appears more clearly in the temporal cross  
163 section of the SR(z) from Zubov lidar, the figure 4 in Nardi et al., (1993), having the vertical axes beginning at 12 km. This  
164 feature may be associated to the combination of what seems to be a downward transport of stratospheric aerosols with the  
165 presence of a thick cirrus cloud attached below. The profiles associated to this feature will be discussed later. The features



166 described above demonstrate that the reproduced  $\alpha_{\text{aer}}(z)$  dataset in the case of Zubov is in reasonable agreement with the reports  
167 in the only two papers available describing the measurements.

168 Figure 1b for Prof. Vize shows in general the same pattern than figure 3 in Avdyushin et al., (1993) although the  $\alpha_{\text{aer}}(z)$   
169 magnitudes in the reproduced dataset are lower. In some way the lack of 9 measurements (~ 45 %) of the 20 reported to be  
170 conducted (Avdyushin et al., 1993) contribute to those low  $\alpha_{\text{aer}}(z)$  magnitudes in the Vize dataset. Also, in figure 1b the  
171 extension of the vertical axes down to the lower level the lidar information was available, 12 km, allows to see aerosols in the  
172 upper troposphere that is not the case in figure 3 in Avdyushin et al., (1993) figure 3.

173

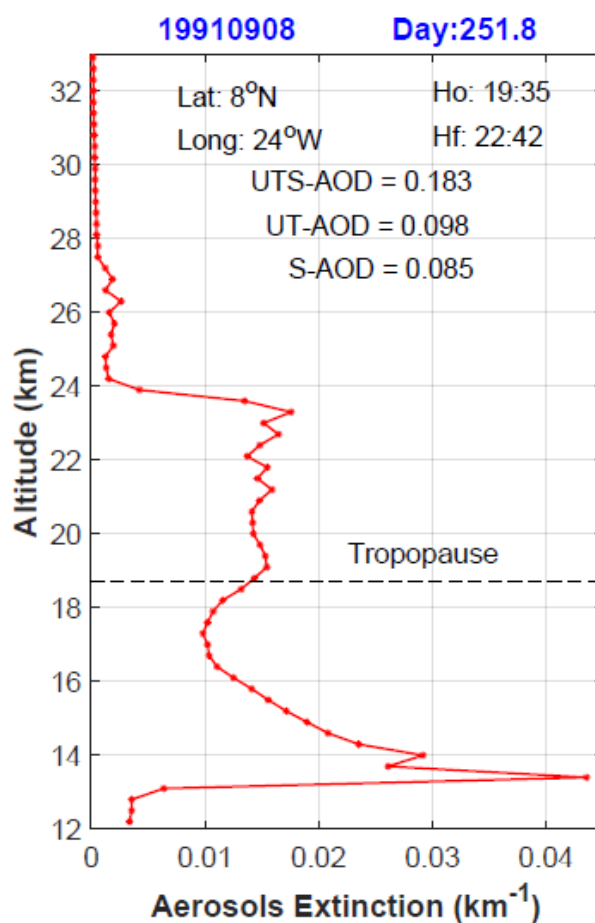
#### 174 **4.2 Downward transport of stratospheric aerosols with a thick cirrus cloud below**

175 The cited area of high values of  $\alpha_{\text{aer}}(z)$  at the tropical middle troposphere in September 1991 around the day 250, shown in the  
176 figure 1a is associated to the  $\alpha_{\text{aer}}(z)$  profile on figure 2 for August 8<sup>h</sup> 1991, at 8°N. The profile of  $\alpha_{\text{aer}}(z)$  extends from 24 km in  
177 the lower stratosphere to 12 km, middle/upper tropical troposphere, across the tropopause located at 18.2 km. The most  
178 plausible explanation of the vertical extension of the layer is the occurrence of stratospheric aerosols downward transport into  
179 the upper and middle troposphere. The figures 2 also includes the values of the total AOD in the upper troposphere and the  
180 lower stratosphere (UTS-AOD) resulting from the contributions of the tropospheric AOD (UT-AOD) 0.087, from 12 km to the  
181 tropopause and the stratospheric AOD (S-AOD) from the tropopause to 33 km. The UT-AOD value of 0.098 and the S-AOD  
182 0.085 have contributions, in the same order of magnitudes, to the UTS-AOD value of 0.183, showing the notable magnitude of  
183 the stratospheric aerosols into the upper and middle troposphere.

184 The figure 2 also show that  $\alpha_{\text{aer}}(z)$  decrease from  $0.012 \text{ km}^{-1}$  at the 18.2 km (tropopause) up to  $0.02 \text{ km}^{-1}$  at 17.3 km and then  
185 increases to ending in two sharp maximums at 14 and 13.4 km with  $\alpha_{\text{aer}}(z)$  of 0.029 and  $0.044 \text{ km}^{-1}$  respectively. This double  
186 peak layer at the bottom of the Pinatubo stratospheric aerosols layer is a cirrus clouds, a phenomenon already reported for the  
187 Pinatubo. Similar lidar  $\beta_{\text{aer}}(z)$  profile structure is reported at Sodankyla (Finland) 66 °N, on figure 1 in Guasta et al., (1994)  
188 for February 3<sup>rd</sup>, 1992. This measurement conducted at Sodankyla was part of the European Arctic Stratospheric Ozone  
189 Experiment (EASOE) campaign during the December 1991 to March 1992 where cirrus clouds were reported in 50% of the 56  
190 measurements conducted. Cirrus were reported to grow often within the stratospheric aerosols layer from Mt Pinatubo as in  
191 the case we are discussing (Guasta et al., 1994). This profile shows, probably, the earlier case of a cirrus observed in lidar  
192 measurements of the Mt Pinatubo stratospheric aerosols.



193 An interesting feature is that in the 48  $\alpha_{\text{aer}}(z)$  profiles from the lidar on Professor Zubov vessel between July and September  
194 1991 only in one profile a cirrus cloud was detected, only 2 % of the profiles. However, in 4 of the 11 available  $\alpha_{\text{aer}}(z)$  profiles  
195 from the lidar on Professor Vize vessel between January and February 1992, 4 profiles showed the presence of cirrus clouds,  
196 around 40% of the observations. These percentage is similar to the reported by a lidar located at Sodankyla, Finland (66 °N),  
197 during the EASOE campaign between December 1991 and March 1992 (Guasta et al., 1994).  
198



199

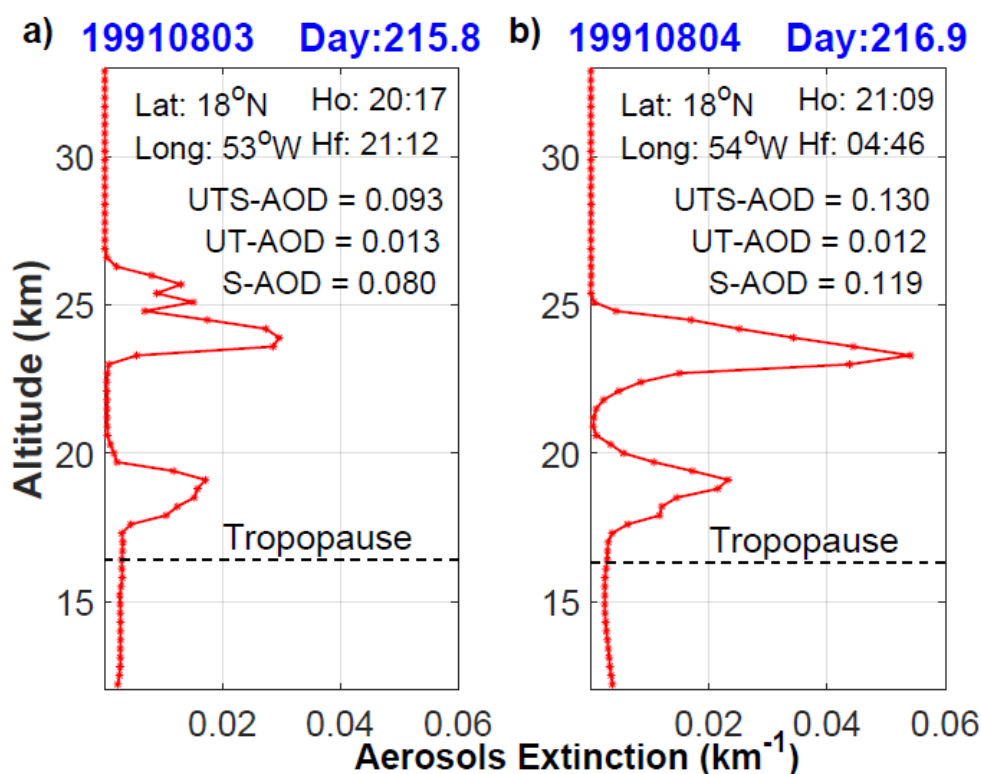
200 **Figure 2: Profile of the  $\alpha_{\text{aer}}(z)$  for September 8<sup>th</sup> at 8 °N, showing the presence of cirrus clouds between 13 and 14 km. It is evident**  
201 **the transport of stratospheric aerosols from the stratosphere into troposphere across the tropopause.**

202



203 **4.3 Absolute maximum  $\alpha_{\text{aer}}(z)$  value:**

204 Figures 3a and b shows the  $\alpha_{\text{aer}}(z)$  profiles on August 3<sup>rd</sup> and 4<sup>th</sup> 1991, the figure 3b belonging to the day the absolute maximum  
205 value of  $\alpha_{\text{aer}}(z)$  was registered and the figure 3a to the day before. Both profiles were taken at the same latitude and only 1°  
206 apart in longitude, allowing to characterize the longitudinal evolution of the Mt. Pinatubo stratospheric aerosols evolution and  
207 variability. A double layer is present both days. The UT-AOD is almost the same for both days but S-AOD in one order of  
208 magnitude from 0.080 on August 3<sup>rd</sup>, 1991 to 0.119 the next day.



209

210 **Figure 3: Profiles of the  $\alpha_{\text{aer}}(z)$  for August 3<sup>rd</sup> and 4<sup>th</sup> at 18 °N.**

211

212 On table 2 the geometrical and optical parameters of the higher and lower layers present in both the August 3<sup>rd</sup> and 4<sup>th</sup>  $\alpha_{\text{aer}}(z)$   
213 profiles. It could be appreciated the altitude descend of both the higher and lower layers from August 3<sup>rd</sup> to 4<sup>th</sup>, with both layers  
214 keeping their depths. The altitude of the  $\alpha_{\text{aer}}(z)$  absolute maximum in the top layer decreased a little more than half a kilometer,  
215 but the maximum in the lower layer maintains its altitude. The magnitudes of the maximums  $\alpha_{\text{aer}}(z)$  in each layer increase, in



216  $2.45 \times 10^{-2} \text{ km}^{-1}$  in the upper layer reaching the absolute maximum value of the entire record and in the lower layer in  $0.62 \times$   
217  $10^{-2} \text{ km}^{-1}$ . The individual layers AOD's increases in 0.028 in the higher layer and 0.023 in the lower. These is an example of  
218 the usefulness of the rescued dataset allowing to quantify those magnitudes during the early stages of the Mount Pinatubo.

219

220 **Table 2. Geometrical and optical parameters of the higher and lower layers present in the August 3<sup>rd</sup> and 4<sup>th</sup>  $\alpha_{\text{aer}}(z)$**   
221 **profiles.**

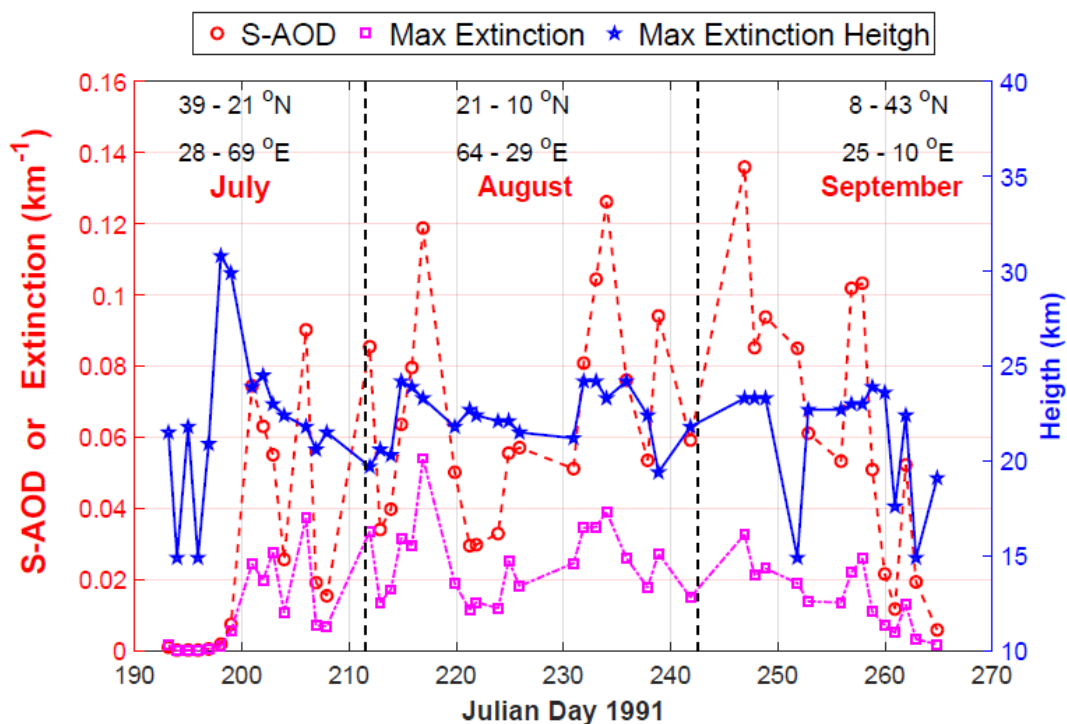
DATE	HIGHER Layer		LOWER Layer	
	19910803	19910804	19910803	19910804
Top [km]	26.6	25.1	20.6	20.9
Base [km]	23.0	21.5	16.4	16.7
$\Delta H$ [km]	3.6	3.6	4.2	4.2
AOD	0.049	0.077	0.031	0.054
Max. $\alpha_{\text{aer}}(z)$ [ $\text{km}^{-1}$ ]	$2.96 \times 10^{-2}$	$5.41 \times 10^{-2}$	$1.71 \times 10^{-2}$	$2.33 \times 10^{-2}$
Max. Height [km]	29.9	29.3	19.1	19.1

222

#### 223 4.4 Evolution of the daily AOD, maximum $\alpha_{\text{aer}}(z)$ and its altitude along the Zubov trajectory

224 Figure 4 shows the temporal evolution, along the entire ship trajectory, of the daily maximum  $\alpha_{\text{aer}}(z)$ , its altitude and S-AOD.  
225 The three months are denoted as the latitudinal and longitudinal bands the lidar sampled during the Zubov trajectory. Daily  
226 maximum  $\alpha_{\text{aer}}(z)$  values are mainly in the range between  $0.0541$  and  $5.7 \times 10^{-5} \text{ km}^{-1}$ , with a mean and standard deviations values  
227 of  $0.018$  and  $0.013 \text{ km}^{-1}$ . The altitudes of the maximum  $\alpha_{\text{aer}}(z)$  values range between  $30.8$  and  $12.2 \text{ km}$ , with mean of  $21.8 \text{ km}$   
228 and standard deviation of  $3.5 \text{ km}$ . The S-AOD mean value is  $0.053$  with a standard deviation of a  $0.037$ , showing its maximum  
229 value of  $0.136$  on September 3<sup>rd</sup> at  $8^\circ \text{N}$  and  $25^\circ \text{E}$ .

230



231

232 **Figure 4: Temporal section of the AOD, maximum extinction and its altitude from the individual lidar profiles measured by Zubov**  
233 **along its trajectory.**

234

## 235 5. Data availability

236 Data described in this work are available at <https://doi.pangaea.de/10.1594/PANGAEA.912770> (Antuña-Marrero et al.,  
237 2020).

238

## 239 6. Summary and outlook

240 Here we present a reproduced version of the stratospheric aerosol extinction profiles derived from lidar measurements  
241 conducted by Professor Zubov and Vize vessels already referenced in the literature (Avdyushin et al., 1993; Nardi et al., 1993)  
242 but unavailable until the present. The data presented consist on two sets of vertical profiles of the  $SR(z)$ ,  $\beta_{aer}(z)$  and  $\alpha_{aer}(z)$  at  
243 300 m vertical resolution, one for each vessel. In the case of Professor Zubov the set include 48 measurement days conducted  
244 between July and September 1991 and for Professor Vize 11 measurements days between January and February 1992.



245 We expect this dataset to contribute to some of the current and future research to simulate the early stages of the Mt Pinatubo  
246 eruption. It will also contribute to a future GloSSAC updates, helping to fill the SAGE II gaps produced by the dense  
247 stratospheric aerosols cloud during the first months after the eruption.

248

249 **Competing Interest:** The authors declare that they have no conflict of interest.

250

#### 251 **Acknowledgements:**

252 These measurements are the result of the scientific cooperation between Roscomhydromet of the former Soviet Union and the  
253 Serviced d' Aeronomie du CNRS of France and the contributions of the authors of the two cited papers and many anonymous  
254 scientists and supporting people. Despite the social and economic upheaval that occurred with the collapse of the former Soviet  
255 Union, this scientific co-operation between Roscomhydromet and CNRS continued. To both agencies, to the authors of the two  
256 cited papers and the anonymous scientists and supporting staff we recognise the value of this continued collaboration and  
257 express our sincere gratitude to all involved. Juan Carlos Antuña-Marrero acknowledges the support by the Copernicus  
258 Atmospheric Monitoring Service (CAMS), one of six services that form Copernicus, the European Union's Earth observation  
259 programme, for his 1-month visit in March 2019 to the School of Earth and Environment, University of Leeds, Leeds, UK. We  
260 are also grateful for funding from the National Centre for Atmospheric Science for Dr. Graham W. Mann via the volcanic  
261 workpackage of the NERC Multi-Centre Long-Term Science Programme on the North Atlantic climate system (ACSIS). We  
262 also acknowledge discussions, during the CAMS-funded visit to Leeds, with Sarah Shallcross and Sandip Dhomse (Univ.  
263 Leeds) in relation to initial model comparisons to the Zubov lidar dataset.

264

#### 265 **References**

266 Avdyushin, S. I., G. F. Tulinov, M. S. Ivanov, B. N. Kuzmenko, I. R. Mezhuev, B. Nardi, A. Hauchecorne and M.-L. Chanin,  
267 1. Spatial and temporal evolution of the optical thickness of the Pinatubo aerosol cloud in the northern hemisphere from a  
268 network of shipborne and stationary lidars. *Geophys. Res. Lett.*, **20**, 1963-1966, 1993.

269 Antuña-Marrero, J. C., Mann, G. W. , Keckhut, P., S. Avdyushin, B. Nardi and L. W. Thomason, Ship borne lidar  
270 measurements in the Atlantic of the 1991 Mt Pinatubo eruption. PANGAEA,  
271 <https://doi.pangaea.de/10.1594/PANGAEA.912770> , 2020. (*Under Review*)



- 272 Antuña, J. C., A. Robock, G. L. Stenchikov, L. W. Thomason, and J. E. Barnes, Lidar validation of SAGE II aerosol  
273 measurements after the 1991 Mount Pinatubo eruption. *J. Geophys. Res.*, **107**(D14), 4194,  
274 <https://doi.org/10.1029/2001JD001441>, 2002.
- 275 Antuña, J. C., A. Robock, G. L. Stenchikov, J. Zhou, C. David, J. E. Barnes and L. W. Thomason, Spatial and temporal  
276 variability of the stratospheric aerosol cloud produced by the 1991 Mount Pinatubo eruption, *J. Geophys. Res.*, **108**(D20), 4624,  
277 <https://doi.org/10.1029/2003JD003722>, 2003.
- 278 Bucholtz, A., Rayleigh-scattering calculations for the terrestrial atmosphere. *App. Opt.*, **34**, p. 2765-2773, 1995.
- 279 Fleming, E. L., Chandra, S., Shoeberl, M. R., Barnett, J. J., Monthly Mean Global Climatology of Temperature, Wind,  
280 Geopotential Height and Pressure for 0-120 km, NASA TM100697, February 1988
- 281 Guasta, M. D., M. Morandi, L. Stefanutti, B. Stein, J. Kolenda, P. Rairoux, J. P. Wolf, R. Matthey, and E. Kyro,  
282 Multiwavelength lidar observation of thin cirrus at the base of the Pinatubo stratospheric layer during the EASOE campaign,  
283 *Geophys. Res. Lett.*, **21**, 1339–1342, 1994.
- 284 McCormick, M. P., and R. E. Veiga, SAGE II measurements of early Pinatubo aerosols, *Geophys. Res. Lett.*, **19**, 155-158,  
285 1992.
- 286 Nardi, B., M.-L. Chanin, A. Hauchecorne, S. I. Avdyushin, G. F. Tulinov, M. S. Ivanov, B. N. Kuzmenko, and I. R. Mezhuev,  
287 Morphology and dynamics of the Pinatubo aerosol layer in the Northern Hemisphere as detected from a ship-borne lidar. Part  
288 II. *Geophys. Res. Lett.*, **20**, 1967–1970, 1993.
- 289 Robock, A.: Volcanic eruptions and climate, *Rev. Geophys.*, 38,191–219, <https://doi.org/10.1029/1998RG000054> , 2000.
- 290 Russell, P. B., T. J. Swissler, and M. P. McCormick, Methodology for error analysis and simulation of lidar aerosol  
291 measurements, *App. Opt.*, **18**, 3783-3797, 1979.
- 292 SSiRC, Activity – Data Rescue <http://www.sparc-ssirc.org/data/datarescueactivity.html> (last access: 2 January 2020), 2020.
- 293 Stratospheric Processes and their Role in Climate (SPARC), Assessment of Stratospheric Aerosol Properties (ASAP), in:  
294 SPARC Report No. 4, edited by: Thomason, L. and Peter, T., *World Climate Research Programme WCRP-124*, WMO/TD No.  
295 1295, WMO, 2006.
- 296 Thomason, L. W., Ernest, N., Millán, L., Rieger, L., Bourassa, A., Vernier, J.-P., Manney, G., Luo, B., Arfeuille, F., and Peter,  
297 T., A global space-based stratospheric aerosol climatology: 1979–2016, *Earth Syst. Sci. Data*, **10**, 469-492,  
298 <https://doi.org/10.5194/essd-10-469-2018> , 2018.
- 299 Timmreck, C.: Modeling the climatic effects of large explosive volcanic eruptions, *Wiley Interdisciplin. Rev.: Clim. Change*,  
300 3, 545–564, <https://doi.org/10.1002/wcc.192> , 2012.